

## Mathieu Functions of Complex Argument and Their Applications to the Scattering by Lossy Elliptic Cylinders

A-K. Hamid

Department of Electrical /Electronics Engineering  
University of Sharjah  
P.O. Box 27272, Sharjah, United Arab Emirates  
email: [akhamid@sharjah.ac.ae](mailto:akhamid@sharjah.ac.ae)

H. A. Ragheb

Department of Electrical Engineering  
King Fahd University of Petroleum and Minerals  
Dhahran, Saudi Arabia

M. I. Hussein

Department of Electrical Engineering  
United Arab Emirates University  
P.O. Box 17555, Al-Ain, United Arab Emirates  
email: [MIHussein@uaeu.ac.ae](mailto:MIHussein@uaeu.ac.ae)

M. Hamid

Department of Electrical and Computer Engineering  
University of South Alabama  
Mobile, Alabama 36688, U.S.A.  
email: [mhamid@usouthal.edu](mailto:mhamid@usouthal.edu)

### Abstract

The aim of this paper is to outline the theory for calculating the angular and radial Mathieu functions of complex arguments. These functions are required for the computation of analytic solutions of electromagnetic scattering by lossy dielectric elliptic cylinders and waveguides. The backscattered echo width of a lossy dielectric elliptic cylinder is compared with the special case of lossy circular and weakly lossy elliptic cylinders and excellent agreement is obtained in all cases. Tabulated and plotted numerical results of typical Mathieu functions are presented.

### 1. Introduction

Many engineering and physics applications involve the solution of structures with elliptical geometries. Analytic solutions to such structures require the computation of angular and radial Mathieu functions in the elliptical coordinate system. Examples of such applications are the solution of elliptical waveguide problems [1-5], optical fibers [6], and elliptical loaded horn and corrugated elliptical horn antennas [2], field prediction inside lossy elliptic cylinders for biological body modeling [7], and scattering by multilayered dielectric elliptic cylinders [8-12]. Furthermore, analytical solutions are generally needed to check the accuracy of numerical or approximate solutions.

Over the years many algorithms and programs have been developed to address the problem of computing Mathieu functions of integer and real arguments [4], [13-22]. However, none of these publications have addressed the more general problem of computing the angular and radial Mathieu functions of complex arguments. Caorsi et. al. have computed the solution of electromagnetic scattering by weakly lossy multilayer elliptic cylinders using first-order truncation of the Taylor expansion of each Mathieu function [23-24]. The same authors have presented the solution of the scattering of an electromagnetic wave by a lossy dielectric elliptic cylinder based on the exact Fourier series solution in

terms of the Mathieu functions with complex argument [24]. Recently, Amendola outlined the theory for the computation of Mathieu functions of complex order by applying the Floquet theory [27]. Unfortunately, there are no numerical results for these functions given in the literature. In this paper, the solution presented in [15] is extended to account for the characteristic values (eigenvalues) of Mathieu functions of complex argument. Once the characteristic values are computed, the complex Fourier coefficients of the Mathieu functions can be obtained. These coefficients are needed to compute the angular and radial Mathieu functions of complex arguments and their derivatives as will be shown.

### 2. Theoretical Background

The homogeneous wave equation (Helmholtz) in elliptical coordinates  $u$ ,  $v$ , and  $z$  is given by

$$\frac{1}{F^2(\cosh^2 u - \cosh^2 v)} \left[ \frac{\partial^2 \psi}{\partial u^2} + \frac{\partial^2 \psi}{\partial v^2} \right] + \left[ \frac{\partial^2}{\partial z^2} + k^2 \right] \psi = 0 \quad (1)$$

The elliptical coordinate system  $(u, v, z)$  is defined in terms of the Cartesian coordinate system  $(x, y, z)$  by  $x = F \cosh(u) \cos(v)$  and  $y = F \sinh(u) \sin(v)$ , where  $F$  is the semifocal length of the elliptical cross section. Assuming no variation of the function  $\psi$  along the  $z$ -axis,

the  $z$ -derivative in (1) will drop out. The resulting differential equation can be separated into the following differential equations in terms of  $U(u)$  and  $V(v)$ . The circumferential (ordinary) Mathieu's differential equation is

$$d^2 V / dv^2 + (a - 2q \cos 2v)V = 0 \quad (2)$$

and the radial (modified) Mathieu's differential equation is

$$d^2 U / du^2 - (a - 2q \cosh 2u)U = 0 \quad (3)$$

where  $q = (kF)^2 = q_R + jq_I$ ,  $k = \omega \sqrt{\mu_1 \epsilon_1}$  and  $\epsilon_1 = \epsilon_1' - j\epsilon_1''$ . It can be shown that there is a countable set of characteristic values of  $a$ , for which the solutions are  $\pi$  or  $2\pi$  periodic.

One can easily distinguish between four kinds of characteristic values (eigenvalues) [15]:

$$a = a_{2r}(q), \text{ even solution, period } \pi$$

$$a = a_{2r+1}(q), \text{ even solution, period } 2\pi$$

$$a = b_{2r+2}(q), \text{ odd solution, period } \pi$$

$$a = b_{2r+1}(q), \text{ odd solution, period } 2\pi$$

$$r = 0, 1, 2, \dots$$

For every characteristic value, the solution of (2) can be given as a Fourier series:

$$Se_{2r}(v, q) = \sum_{m=0}^{\infty} A_{2m}^{2r} \cos 2mv \tag{4a}$$

$$Se_{2r+1}(v, q) = \sum_{m=0}^{\infty} A_{2m+1}^{2r+1} \cos(2m+1)v \tag{4b}$$

$$So_{2r+2}(v, q) = \sum_{m=0}^{\infty} B_{2m+2}^{2r+2} \sin(2m+2)v \tag{4c}$$

$$So_{2r+1}(v, q) = \sum_{m=0}^{\infty} B_{2m+1}^{2r+1} \sin(2m+1)v \tag{4d}$$

Where the  $A$ 's and  $B$ 's are complex Fourier coefficients. For computing the Fourier coefficients, one has to obtain first the characteristic values.

Substitution of the series (4a), (4b), (4c), and (4d) in the differential equation (2), yields four sets of equations for computing the Fourier coefficients:

$$\begin{bmatrix} a_{2r} - q & 0 & & & & \\ -2q & a_{2r} - 4 & -q & & & \\ 0 & & \ddots & & & \\ & & & \ddots & & \\ & & & & -q & \\ & & & & & 0 \\ & & & & & & -q & a_{2r} - (2m)^2 \end{bmatrix} \begin{bmatrix} A_0^{2r} \\ A_2^{2r} \\ \vdots \\ A_{2m}^{2r} \end{bmatrix} = 0 \tag{5a}$$

$$\begin{bmatrix} a_{2r+1} - 1 - q & -q & 0 & & & \\ -q & a_{2r+1} - 9 & -q & & & \\ 0 & & \ddots & & & \\ & & & \ddots & & \\ & & & & -q & \\ & & & & & 0 \\ & & & & & & -q & a_{2r+1} - (2m+1)^2 \end{bmatrix} \begin{bmatrix} A_1^{2r+1} \\ A_3^{2r+1} \\ \vdots \\ A_{2m+1}^{2r+1} \end{bmatrix} = 0 \tag{5b}$$

$$\begin{bmatrix} b_{2r+2} - 4 & -q & 0 & & & \\ -q & b_{2r+2} - 16 & -q & & & \\ 0 & & \ddots & & & \\ & & & \ddots & & \\ & & & & -q & \\ & & & & & 0 \\ & & & & & & -q & b_{2r+2} - (2m+2)^2 \end{bmatrix} \begin{bmatrix} B_2^{2r+2} \\ B_4^{2r+2} \\ \vdots \\ B_{2m+2}^{2r+2} \end{bmatrix} = 0 \tag{5c}$$

$$\begin{bmatrix} b_{2r+1} - 1 - q & -q & 0 & & & \\ -q & b_{2r+1} - 9 & -q & & & \\ 0 & & \ddots & & & \\ & & & \ddots & & \\ & & & & -q & \\ & & & & & 0 \\ & & & & & & -q & b_{2r+1} - (2m+2)^2 \end{bmatrix} \begin{bmatrix} B_1^{2r+1} \\ B_3^{2r+1} \\ \vdots \\ B_{2m+1}^{2r+1} \end{bmatrix} = 0 \tag{5d}$$

We shall now show the computation of  $a_{2r+1}$  in (5b). All other characteristic values can be calculated in exactly the same way. It is clear from (5b) that  $a_{2r+1}$  can be seen as the eigenvalues of the infinite tridiagonal matrix,

$$\begin{bmatrix} 1+q & q & 0 & & & \\ q & 9 & q & & & \\ 0 & & \ddots & & & \\ & & & \ddots & & \\ & & & & q & \\ & & & & & 0 \\ & & & & & & q & (2m+1)^2 \end{bmatrix} \tag{6}$$

In calculating the eigenvalues and Fourier coefficients, it is necessary to truncate the matrix after a finite number of columns and rows to obtain the required accuracy.

Once the coefficients  $A_{2m}^{2r}, A_{2m+1}^{2r+1}, B_{2m+2}^{2r+2}, B_{2m+1}^{2r+1}$  are determined using the routine DEVCCG from Microsoft IMSL Math Libraries, the angular Mathieu functions in equations (4) as well as their respective derivatives can be calculated. Next, we compute the radial Bessel functions of the first and second types using equation (3) along with the previously computed Fourier coefficients. The equations used for the computation of the even and odd functions of the first type are

$$J_{e2r}(u, q) = (-1)^r \sqrt{\pi/2} \sum_{m=0}^M (-1)^m A_{2m}^{2r} J_m(x_1) J_m(x_2) / A_0^{2r} \tag{7}$$

$$J_{e2r+1}(u, q) = (-1)^r \sqrt{\pi/2} \sum_{m=0}^M (-1)^m A_{2m+1}^{2r+1} [J_{m+1}(x_1) J_m(x_2) + J_m(x_1) J_{m+1}(x_2)] / A_1^{2r+1} \tag{8}$$

$$J_{o2r}(u, q) = (-1)^r \sqrt{\pi/2} \sum_{m=1}^M (-1)^m B_{2m}^{2r} [J_{m+1}(x_1) J_{m-1}(x_2) - J_{m+1}(x_1) J_{m-1}(x_2)] / B_2^{2r} \tag{9}$$

$$J_{o2r+1}(u, q) = (-1)^r \sqrt{\pi/2} \sum_{m=0}^M (-1)^m B_{2m+1}^{2r+1} [J_{m+1}(x_1) J_m(x_2) - J_m(x_1) J_{m+1}(x_2)] / B_1^{2r+1} \tag{10}$$

where  $x_1 = \frac{\sqrt{q}}{2} e^u, x_2 = \frac{\sqrt{q}}{2} e^{-u}$ . By replacing  $J_m$  by  $Y_m$ ,

we obtain the even and odd radial functions of the second type as follows

$$Y_{e2r}(u, q) = (-1)^r \sqrt{\pi/2} \sum_{m=0}^M (-1)^m A_{2m}^{2r} Y_m(x_1) J_m(x_2) / A_0^{2r} \tag{11}$$

$$Y_{e2r+1}(u, q) = (-1)^r \sqrt{\pi/2} \sum_{m=0}^M (-1)^m A_{2m+1}^{2r+1} [Y_{m+1}(x_1) J_m(x_2) + Y_m(x_1) J_{m+1}(x_2)] / A_1^{2r+1} \tag{12}$$

$$Y_{o2r}(u, q) = (-1)^r \sqrt{\pi/2} \sum_{m=1}^M (-1)^m B_{2m}^{2r} [Y_{m+1}(x_1) J_{m-1}(x_2) - J_{m+1}(x_1) Y_{m-1}(x_2)] / B_2^{2r} \tag{13}$$

$$Y_{o2r+1}(u, q) = (-1)^r \sqrt{\pi/2} \sum_{m=0}^M (-1)^m B_{2m+1}^{2r+1} [Y_{m+1}(x_1) J_m(x_2) - J_m(x_1) J_{m+1}(x_2)] / B_1^{2r+1} \tag{14}$$

Numerical results for the derivatives, with respect to  $q$ , of the even and odd angular and radial Mathieu functions are obtained using the equations given in [14-17].

### 3. Electromagnetic Scattering by a Lossy Dielectric Elliptic Cylinder

Consider the case of a linearly polarized electromagnetic plane wave incident on a lossy dielectric elliptic cylinder (of permeability  $\mu$ , permittivity  $\varepsilon$  and conductivity  $\sigma$ ) at an angle  $\phi_i$  measured with respect to the  $x$  axis as shown in [25]. The electric field component of the TM polarized plane wave of amplitude  $E_0$  is given by

$$E_z^i = E_0 e^{jk_0 \rho \cos(\phi - \phi_i)} \quad (15)$$

where  $k_0$  is the wave number in free space. The incident electric field may be expressed in terms of Mathieu functions as follows

$$E_z^i = \sum_{m=0}^{\infty} A_{em} R_{em}^{(1)}(c_0, \xi) S_{em}(c_0, \eta) + \sum_{m=1}^{\infty} A_{om} R_{om}^{(1)}(c_0, \xi) S_{om}(c_0, \eta) \quad (16)$$

$$A_{om} = E_0 j^m \frac{\sqrt{8\pi}}{N_{om}(c_0)} S_{om}(c_0, \cos \phi_i) \quad (17)$$

$$N_{om}(c) = \int_0^{2\pi} [S_{om}(c, \eta)]^2 dv \quad (18)$$

where  $\xi = \cosh u$  and  $\eta = \cos v$ ,  $c_0 = k_0 F$ ,  $F$  is the semifocal length of the elliptical cross section,  $S_{em}$ , while  $S_{om}$  are the even and odd angular Mathieu functions of order  $m$ , respectively,  $R_{em}^{(1)}$  and  $R_{om}^{(1)}$  are the even and odd radial Mathieu functions of the first kind, and  $N_{em}$  and  $N_{om}$  are the even and odd normalized functions.

Electric field expansion inside and outside the lossy dielectric cylinder can be obtained by solving the Helmholtz equation in the elliptical coordinate system using the separation of variables technique. The scattered electric field outside the elliptic cylinder for ( $\xi > \xi_1$ ) can be expressed in terms of a sum series of Mathieu and modified Mathieu functions as follows

$$E_z^s = \sum_{m=0}^{\infty} B_{em} R_{em}^{(4)}(c_0, \xi) S_{em}(c_0, \eta) + \sum_{m=1}^{\infty} B_{om} R_{om}^{(4)}(c_0, \xi) S_{om}(c_0, \eta) \quad (19)$$

where  $B_{em}$  and  $B_{om}$  are the unknown scattered field expansion coefficients,  $R_{em}^{(4)}$  and  $R_{om}^{(4)}$  are the even and odd modified Mathieu functions of the fourth kind. Similarly, the transmitted electric field inside the cylinder for  $\xi < \xi_1$  can be written as

$$E_z^t = \sum_{m=0}^{\infty} C_{em} R_{em}^{(1)}(c_1, \xi) S_{em}(c_1, \eta) + \sum_{m=1}^{\infty} C_{om} R_{om}^{(1)}(c_1, \xi) S_{om}(c_1, \eta) \quad (20)$$

where  $c_1 = k_1 F$  is complex, and  $k_1 = \omega \sqrt{\mu_1 \varepsilon_1}$ .  $\varepsilon_1 = \varepsilon_1' - j\varepsilon_1''$ ,  $C_{em}$  and  $C_{om}$  are the unknown transmitted field expansion coefficients. The magnetic field component inside and outside the cylinder can be obtained using Maxwell's equations, i.e.

$$H_u = \frac{-j}{\omega \mu_1 h} \frac{\partial E_z}{\partial v} \quad (21)$$

$$H_v = \frac{-j}{\omega \mu_1 h} \frac{\partial E_z}{\partial u} \quad (22)$$

$$h = F \sqrt{\cosh^2 u - \cos^2 v} \quad (23)$$

The unknown expansion coefficients can be obtained by imposing the continuity of the tangential field components at surface of the cylinder  $\xi = \xi_1$ , i.e.

$$\sum_{m=0}^{\infty} M_{enm}(c_1, c_0) B_{em} \left[ \mu_r R_{em}^{(4)'}(c_0, \xi_1) - R_{em}^{(4)}(c_0, \xi_1) \frac{R_{en}^{(1)'}(c_1, \xi_1)}{R_{en}^{(1)}(c_1, \xi_1)} \right] = \sum_{m=0}^{\infty} M_{enm}(c_1, c_0) A_{em} \left[ R_{em}^{(1)}(c_0, \xi_1) \frac{R_{en}^{(1)'}(c_1, \xi_1)}{R_{en}^{(1)}(c_1, \xi_1)} - \mu_r R_{em}^{(1)'}(c_0, \xi_1) \right] \quad (24)$$

$$\sum_{m=1}^{\infty} M_{onm}(c_1, c_0) B_{om} \left[ \mu_r R_{om}^{(4)'}(c_0, \xi_1) - R_{om}^{(4)}(c_0, \xi_1) \frac{R_{on}^{(1)'}(c_1, \xi_1)}{R_{on}^{(1)}(c_1, \xi_1)} \right] = \sum_{m=0}^{\infty} M_{onm}(c_1, c_0) A_{om} \left[ R_{om}^{(1)}(c_0, \xi_1) \frac{R_{on}^{(1)'}(c_1, \xi_1)}{R_{on}^{(1)}(c_1, \xi_1)} - \mu_r R_{om}^{(1)'}(c_0, \xi_1) \right] \quad (25)$$

$$M_{onm}(c_0, c_1) = \int_0^{2\pi} S_{em}(c_1, \eta) S_{om}(c_0, \eta) dv \quad (26)$$

where  $\mu_r$  is the relative permeability of the dielectric region. The TE scattering by a lossy elliptic cylinder is also presented. In this case a derivation dual to that of the TM case leads to the following solution [25]

$$\sum_{m=0}^{\infty} M_{enm}(c_1, c_0) B_{em}^{TE} \left[ \varepsilon_r R_{em}^{(4)'}(c_0, \xi_1) - R_{em}^{(4)}(c_0, \xi_1) \frac{R_{en}^{(1)'}(c_1, \xi_1)}{R_{en}^{(1)}(c_1, \xi_1)} \right] = \sum_{m=0}^{\infty} M_{enm}(c_1, c_0) A_{em} \left[ R_{em}^{(1)}(c_0, \xi_1) \frac{R_{en}^{(1)'}(c_1, \xi_1)}{R_{en}^{(1)}(c_1, \xi_1)} - \varepsilon_r R_{em}^{(1)'}(c_0, \xi_1) \right] \quad (27)$$

$$\sum_{m=1}^{\infty} M_{onm}(c_1, c_0) B_{om}^{TE} \left[ \varepsilon_r R_{om}^{(4)'}(c_0, \xi_1) - R_{om}^{(4)}(c_0, \xi_1) \frac{R_{on}^{(1)'}(c_1, \xi_1)}{R_{on}^{(1)}(c_1, \xi_1)} \right] = \sum_{m=0}^{\infty} M_{onm}(c_1, c_0) A_{om} \left[ R_{om}^{(1)}(c_0, \xi_1) \frac{R_{on}^{(1)'}(c_1, \xi_1)}{R_{on}^{(1)}(c_1, \xi_1)} - \varepsilon_r R_{om}^{(1)'}(c_0, \xi_1) \right] \quad (28)$$

The scattered near and far fields for the TM and TE cases can be calculated once the scattered fields expansion coefficients are known. The far scattered field expressions can be obtained as follows

$$E_z^s = \sqrt{\frac{j}{k_0 \rho}} e^{-jk_0 \rho} \sum_m j^m [B_{em}^{TM} S_{em}(c_0, \eta) + B_{om}^{TM} S_{om}(c_0, \eta)] \quad (29)$$

$$H_z^s = \sqrt{\frac{j}{k_0 \rho}} e^{-jk_0 \rho} \sum_m j^m [B_{em}^{TE} S_{em}(c_0, \eta) + B_{om}^{TE} S_{om}(c_0, \eta)] \quad (30)$$

Far Field data are usually expressed in terms of the scattering cross section per unit length, *i.e.*, the echo width. For the TM polarization case it is defined as

$$\sigma_{TM} = 2\pi\rho \lim_{\rho \rightarrow \infty} \frac{|E_z^s|^2}{|E_z^i|^2} \quad (31)$$

Eq. (30) can be put in simpler form for the purpose of computation as follows

$$\sqrt{\frac{\sigma_{TM}}{\lambda}} = \sum_m j^m [B_{em} S_{em}(c_0, \eta) + B_{om} S_{om}(c_0, \eta)] \quad (32)$$

#### 4. Numerical Results

To determine the accuracy of the computer program, the Fourier expansion coefficients of Mathieu functions are computed. These results are in excellent agreement with those given in [16] for the case of real positive argument  $q$ , and the maximum difference was found to be  $10^{-5}$ . Also, to verify the accuracy of the computer program for the case of complex argument  $q$ , we solved the problem of electromagnetic scattering by a lossy dielectric elliptic cylinder since no results are available in the literature. The computed numerical results were compared with the special case of scattering by a lossy circular dielectric cylinder, and with electromagnetic scattering by weakly lossy multilayer elliptic cylinder [23,26]. Fig. 1 shows the numerical results of the scattered normalized echo width  $\sigma$  of a lossy dielectric circular cylinder having a relative permittivity of  $\epsilon_r = 1 - j11.3$  and electrical radius  $k_0 a = 3.33$  for TM and TE polarizations. These results compare very well with those presented in [26]. In this case the circular cylinder was approximated using an axial ratio close to 1, and was excited by an incident plane wave with  $\phi_i = 180^\circ$ .

Fig. 2 compares the back scattering normalized echo width  $k_0 \sigma(0)/4$  for a homogeneous elliptical cylinder with axial ratio  $a/b = 2$  and  $\epsilon' = 4.0$ . Two cases are studied; these are the lossless cylinder case with  $\epsilon'' = 0.0$  and a weak loss cylinder case where  $\epsilon'' = 0.6$ . The calculated results are in very good agreement with those published in [23]. One can easily recognize the reduction in the back scattering normalized echo width due to the presence of a small loss. This can be attributed to the fact that the weak loss material absorbed part of the incident wave energy. Another clear observation is the shift in of resonance location. For a free loss material, resonance is observed around  $k_0 a = 3.6$ , while in the weak loss case the resonance has shifted to around

$k_0 a = 2.1$ . Fig. 3 illustrates the results obtained in [16] for the radial Mathieu function of the first kind and zero order with respect to  $u$  for different values of  $q$ , and presented here to validate the accuracy of the computer code. Finally, Figs. 4-13 present a collection of data for Mathieu functions (radial and angular) of complex arguments. The Fourier expansion coefficients of Mathieu functions for different arguments are tabulated in Tables 1-4. These results should be very helpful for researchers solving problems in the elliptic coordinate system.

#### 5. Conclusions

The theory for calculating the angular and radial Mathieu functions of complex arguments has been outlined. The computed backscattered echo width of a lossy dielectric elliptic cylinder was compared with the special case of lossy circular and weakly lossy elliptic cylinders and the results are in complete agreement. Selected numerical results for Mathieu functions are plotted and tabulated for limited ranges due to limitation on space.

#### ACKNOWLEDGEMENT

The authors wish to acknowledge the support provided by the University of Sharjah, the United Arab Emirates University and the University of South Alabama. Also the first and third authors wish to acknowledge King Fahd University of Petroleum and Minerals in Saudi Arabia where the special case of Mathieu Functions of real argument was treated in a project entitled "Propagation and Radiation from Elliptical Waveguide Partly Filled with Nonconfocal Dielectric," by H. Ragheb and A-K. Hamid, 2000.

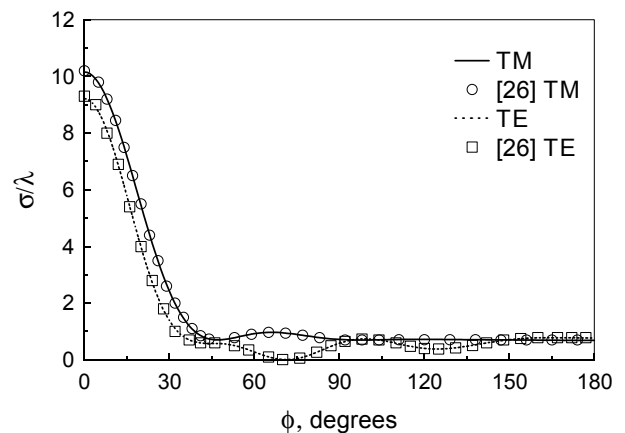


Figure 1: TM and TE Normalized backscattered echo width versus  $\phi$  of a lossy circular cylinder with  $k_0 a = 3.33$  and  $\epsilon_r = 1 - j11.3$ .

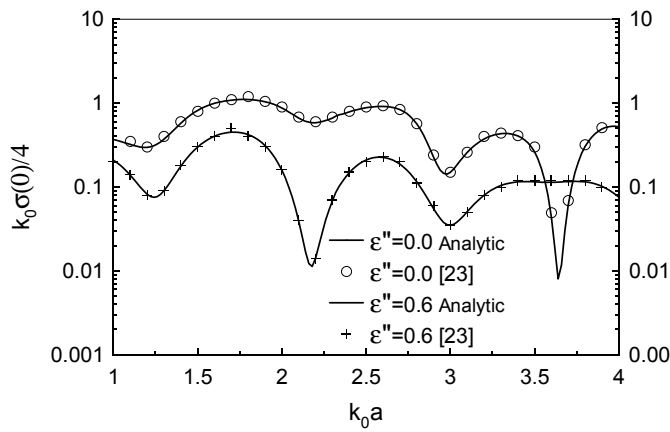


Figure 2: TM Normalized backscattered echo width versus  $\phi$  of a lossy dielectric elliptic cylinder with  $\epsilon_r = 4$ ,  $a/b=2$  and  $\phi_i = 0^\circ$

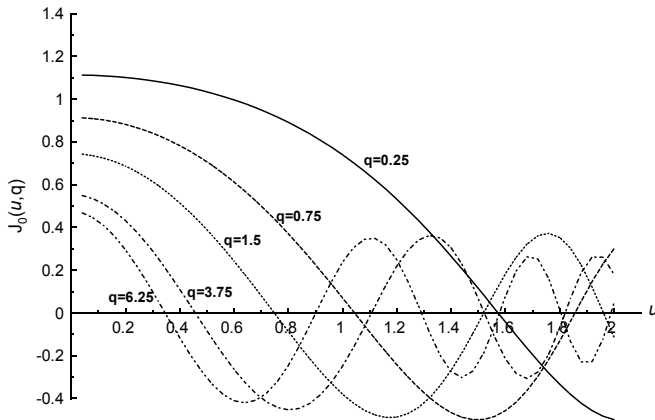


Figure 3: Radial Mathieu function of the first kind and zero order vs  $u$  for different values of  $q$ .

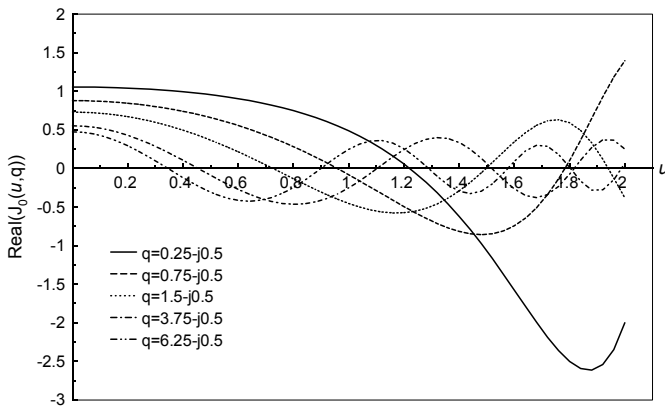


Figure 4: Real part of the radial Mathieu function of the first kind and zero order vs  $u$  for different values of complex  $q$ .

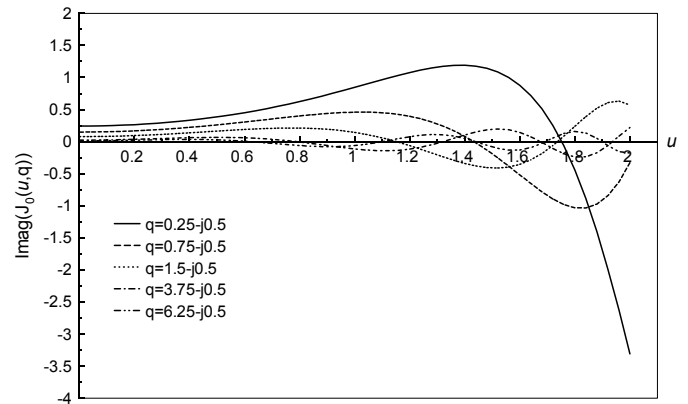


Figure 5: Imaginary part of radial Mathieu function of the first kind and zero order vs  $u$  for different values of  $q$ .

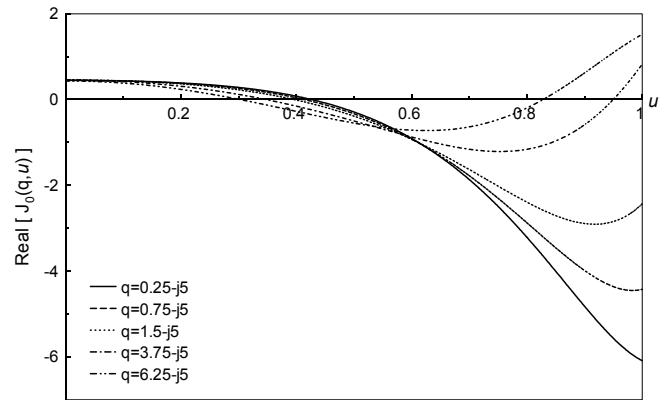


Figure 6: Real part of the radial Mathieu function of the first kind and zero order vs  $u$  for different values of  $q$ .

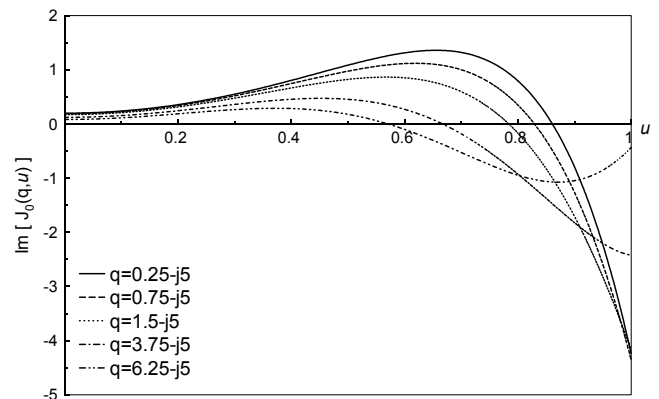


Figure 7: Imaginary part of the radial Mathieu function of the first kind and zero order vs  $u$  for different values of complex  $q$ .

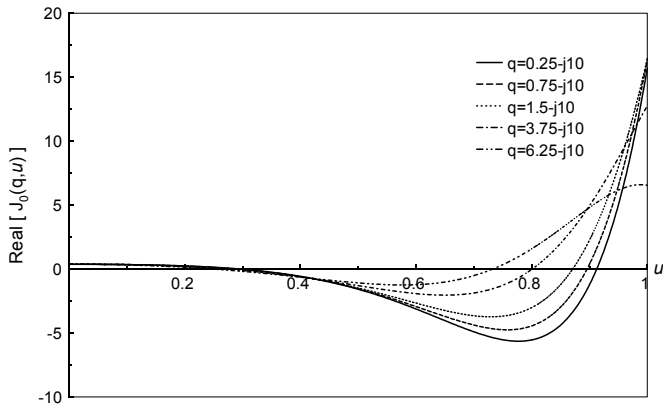


Figure 8: Real part of the radial Mathieu function of the first kind and zero order vs  $u$  for different values of  $q$ .

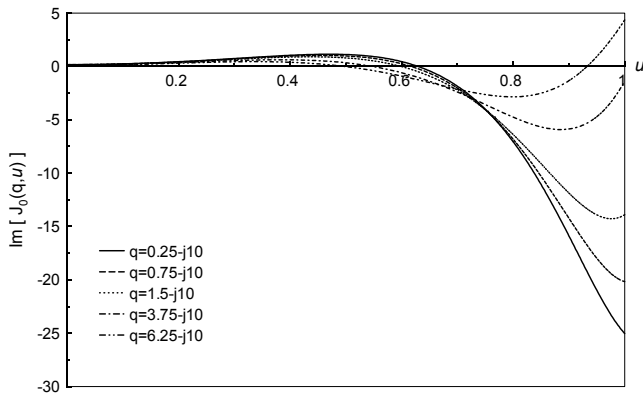


Figure 9: Imaginary part of the radial Mathieu function of the first kind and zero order vs  $u$  for different values of  $q$ .

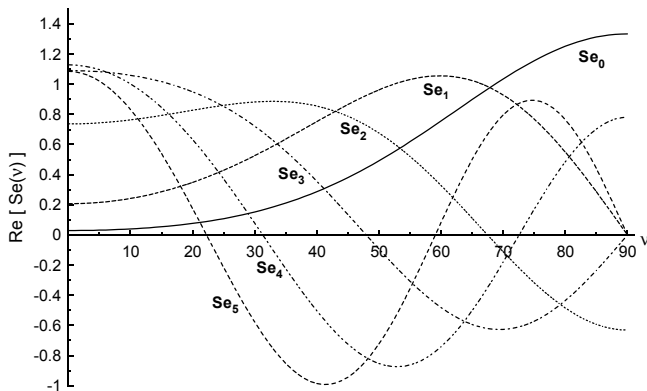


Figure 10: Real part of even periodic Mathieu function with orders 0-5 and  $q = 5 - j2$  vs  $v$ .

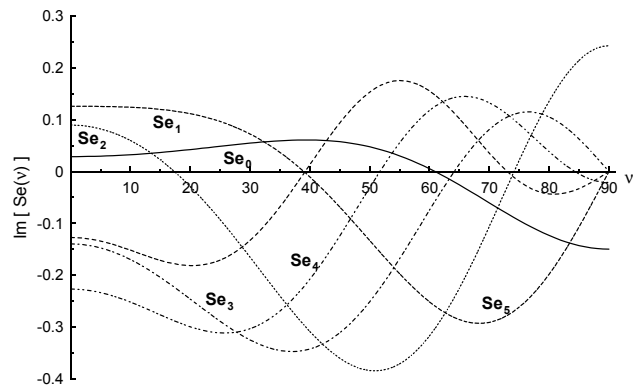


Figure 11: Imaginary part of even periodic Mathieu function with orders 0-5 and  $q = 5 - j2$  vs  $v$ .

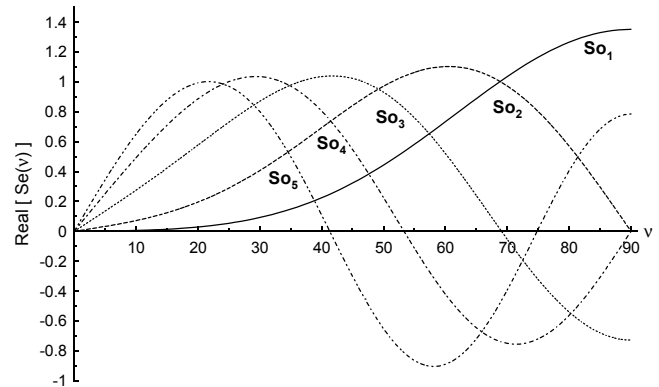


Figure 12: Real part of odd periodic Mathieu function with orders 1-5 and  $q = 5 - j5$  vs  $v$ .

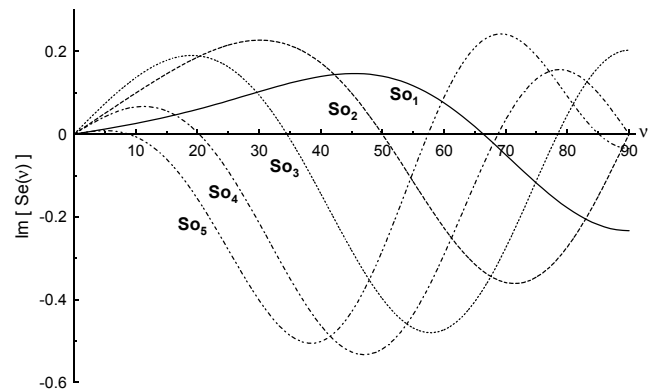


Figure 13: Imaginary part of odd periodic Mathieu function with orders 1-5 and  $q = 5 - j5$  vs  $v$ .

Table 1: Complex Fourier expansion coefficients of even-even Mathieu function ( $A_{2m}^{2r}$ )

		$A_{2m}^{2r}$			
		0		2	
$q = 5 + j0$	$m \setminus r$	Real	Imag.	Real	Imag.
	0	0.540612446	0	0.438737166	0
	2	-0.627115413	0	0.65364026	0
	4	0.14792709	0	-0.426578935	0
	6	-0.017848061	0	0.075885673	0
$q = 5 + j5$					
	0	0.49810151	0	0.314442843	0.171487341
	2	-0.662750285	-0.130176082	0.604942355	0
	4	0.168770876	0.133382581	0.026159729	-0.59020582
	6	-0.010394981	-0.034782531	-0.140969223	0.089859201
$q = 10 + j10$					
	0	-0.44951258	0.056260383	-0.294924019	0.029961136
	2	0.694591697	0	-0.059497099	0.255064311
	4	-0.296630326	-0.105862211	0.746844887	0
	6	0.058531831	0.064924524	-0.323904602	-0.281747705

Table 3: Complex Fourier expansion coefficients of odd-even Mathieu function ( $B_{2m}^{2r}$ )

		$B_{2m}^{2r}$			
		2		10	
$q = 5 + j0$	$m \setminus r$	Real	Imag.	Real	Imag.
	2	0.933429442	0	0.000033444	0
	4	-0.354803915	0	0.000642976	0
	6	0.052963729	0	0.010784806	0
	8	-0.004295885	0	0.13767512	0
$q = 5 + j5$					
	2	0.870294564	0	-0.000130329	-0.000002685
	4	-0.396630117	-0.272694975	-0.001280155	0.001222013
	6	0.028211436	0.099835145	-0.000421242	0.021019319
	8	0.0053059	-0.01083967	0.132565552	0.136516812
$q = 10 + j10$					
	2	0.734255554	0	-0.001900098	-0.000156527
	4	-0.580164625	-0.25100546	-0.009959144	0.008264692
	6	0.137051442	0.19916337	-0.006136282	0.076604876
	8	0.002015162	-0.052591626	0.231256474	0.260037365

Table 2: Complex Fourier expansion coefficients of even-odd Mathieu function ( $A_{2m+1}^{2r+1}$ )

		$A_{2m+1}^{2r+1}$			
		1		3	
$q = 5 + j0$	$m \setminus r$	Real	Imag.	Real	Imag.
	1	0.762463687	0	0.077685798	0
	3	-0.63159632	0	0.30375103	0
	5	0.139684806	0	0.927728396	0
	7	-0.014915596	0	-0.201706148	0
$q = 5 + j5$					
	1	-0.517275706	0.286011205	-0.041658559	0.131675807
	3	0.765785524	0	0.239854654	0.290697818
	5	-0.197812838	-0.153451695	0.878673205	0
	7	0.007517743	0.03807304	-0.166961766	-0.194677341
$q = 10 + j10$					
	1	-0.433393417	0.130050198	0.666818493	0
	3	0.775016392	0	0.494260893	-0.299695541
	5	-0.373034841	-0.201569455	-0.01872188	-0.426395143
	7	0.054220182	0.106990887	-0.184358865	0.054869005

Table 4: Complex Fourier expansion coefficients of odd-odd Mathieu function ( $B_{2m+1}^{2r+1}$ )

		$B_{2m+1}^{2r+1}$			
		1		3	
$q = 5 + j0$	$m \setminus r$	Real	Imag.	Real	Imag.
	1	0.940019022	0	0.050382462	0
	3	-0.336541963	0	0.297365513	0
	5	0.055477529	0	0.931566996	0
	7	-0.005089553	0	-0.202193639	0
$q = 5 + j5$					
	1	0.904373155	0	0.016113831	0.092448918
	3	-0.389707951	-0.145292103	0.268912553	0.288134908
	5	0.057923929	0.074976514	0.876555541	0
	7	-0.000091975	-0.012224892	-0.16648902	-0.196783024
$q = 10 + j10$					
	1	0.852110863	0	-0.043283898	0.203330605
	3	-0.460992769	-0.18202088	0.234907973	0.510680316
	5	0.083408677	0.142179121	0.741126923	0
	7	0.009774806	-0.031241645	-0.081180316	-0.285889059



**A.-K. Hamid** was born in Tulkarm, WestBank, on Sept. 9, 1963. He received the B.Sc. degree in Electrical Engineering from West Virginia Tech, West Virginia, U.S.A. in 1985. He received the M.Sc. and Ph.D. degrees from the university of Manitoba, Winnipeg, Manitoba, Canada in 1988 and 1991, respectively, both in Electrical Engineering. From 1991-

1993, he was with Quantic Laboratories Inc., Winnipeg, Manitoba, Canada, developing two and three dimensional electromagnetic field solvers using boundary integral method. From 1994-2000 he was with the faculty of electrical engineering at King Fahd University of Petroleum and Minerals, Dhahran, Saudi Arabia. Since Sept. 2001 he is an associate Prof. in the electrical/electronics and computer engineering at the University of Sharjah, Sharjah, United Arab Emirates. His research interest includes EM wave scattering from two and three dimensional bodies, propagation along waveguides with discontinuities, FDTD simulation of cellular phones, and inverse scattering using neural networks.



**Mousa I. Hussein** received the B.Sc. degree in electrical engineering from West Virginia Tech, USA, 1985, M.Sc. and Ph.D. degrees from University of Manitoba, Winnipeg, MB, Canada, in 1992 and 1995, respectively, both in electrical engineering. From 1995 to 1997, he was with research and development

group at Integrated Engineering Software Inc., Winnipeg, Canada, working on developing EM specialized software based on the Boundary Element method. In 1997 he joined faculty of engineering at Amman University, Amman, Jordan, as an Assistant Professor. He is currently with the Electrical Engineering Dept. at the United Arab Emirates University. Dr. Hussein current research interests includes, computational electromagnetics, electromagnetic scattering, antenna analysis and design, EMI and signal integrity.

**Hassan Ragheb** was born in Port-Said, Egypt, in 1953. He received the B. Sc. Degree in Electrical Engineering from Cairo University, Egypt, in 1977 and the M. Sc. and Ph. D. degrees in Electrical Engineering from the University of Manitoba, Winnipeg, Canada, in 1984 and 1987, respectively. From 1987 to 1989, he was a research assistant in the Department of Electrical Engineering, University of Manitoba. In 1989, he joined the Department of Electrical Engineering at the King Fahd University of Petroleum and Minerals, where he is now an Associate Professor of Electrical Engineering. His research interests include electromagnetic scattering by multiple and coated objects,

microstrip antennas, phased arrays, slot and open ended waveguide antennas.



**Michael Hamid** Graduated from McGill University in Montreal with a B.Eng. degree in 1960, a M.Eng. degree in 1962 and from the University of Toronto with a Ph.D. degree in 1966, all in Electrical Engineering. He joined the University of Manitoba in 1965 where he became a Professor of Electrical Engineering and head of the Antenna Laboratory.

He was a Visiting Professor at the Universities of California Davis and Central Florida and is presently a Professor of Electrical Engineering at the University of South Alabama. He is a past president of the International Microwave Power Institute, a Fellow of IEE and IEEE and published 307 referred articles and 25 patents.

## References

1. Kretzchmar, J. G., "Wave propagation in conducting elliptical waveguides," IEEE Trans. Microwave Theory Tech., vol. MTT-18, pp. 547-554, 1970.
2. Clarricoats, P. J. B., and Olver, A. D., "Corrugated Horns for Microwave Antennas," Stevenage, U.K., Peregrinus, 1984.
3. Matras, P., Bunger, R., and Arndt, F., "Analysis of the step discontinuity in elliptical waveguides," IEEE Microwave Guided Wave Lett., vol. 6, pp. 143-145, Mar., 1996.
4. Schneider, M., Marquardt, J., "Fast Computation of Modified Mathieu Functions Applied to Elliptical Waveguide Problems," IEEE Trans. Microwave Theory Tech., vol. 47, pp. 513-515, 1999.
5. James. L. G., "Propagation and Radiation from partly filled elliptical waveguide," Proc. IEE, vol. 136, pt. H, pp. 195-201, June 1989.
6. Dyott, R. B., "Elliptical Fiber waveguides," Norwood, MA, Artech House, 1995.
7. Caorsi, S, Pastorino, M., and Raffetto, M, "EM Field Prediction Inside Lossy Multilayer Elliptic Cylinders for Biological-Body Modeling and Numerical-Procedure Testing," IEEE Trans. Biomedical Eng., Vol. 11, pp. 1304-1309, 1999.
8. Sebak, A-R., "Scattering from dielectric coated impedance elliptic cylinder," IEEE Trans. On Antenna and Prog., vol. 48, pp. 1574-1580, 2000.
9. R. Holand and V.P. Cable, "Mathieu functions and their applications to scattering by a coated strip," IEEE Trans. On Elect. Compt., vol. 34, no. 1, pp. 9-16, 1992.
10. Caorsi, S, Pastorino, M., and Raffetto, M., "Electromagnetic scattering by a multilayer elliptic cylinder under transverse-magnetic illumination: series



- solution in terms of Mathieu function," *IEEE Trans. On Antenna and Propag.*, vol. 45, no. 6, pp. 926-935, 1997.
11. Sebak, A., Shafai, L., and Ragheb, H., "Electromagnetic scattering by a two layered piecewise homogeneous confocal elliptic cylinder," *Radio Science*, vol. 26, pp. 111-119, 1991.
  12. Kim, S.K., and Yeh, C., "Scattering of an obliquely incident wave by a multilayered elliptical lossy dielectric cylinder," *Radio Science*, vol. 26, pp. 1165-1176, 1991.
  13. Rengarajan, S.R., and Lewis, J.E., "Mathieu functions of integral order and real arguments," *IEEE Trans. Microwave Theory Tech.*, vol. MTT-28, pp. 276-277, 1980.
  14. Toyama, N., and Shogen, K., "Computation of the value of the even and odd Mathieu functions of order N for a given parameter S and argument X," *IEEE Trans. On Antennas and Propag.*, vol. AP-32, pp. 537-539, 1984.
  15. "The "Numerical analysis" Group" at Delft University of Technology, "On the computation of Mathieu functions," *Journal of Engineering Mathematics*, vol. 7, pp. 39-61, 1973.
  16. Abramowitz, M., and Stegun, I., *Handbook of Mathematical Functions N.B.S, Applied Mathematical series 55*, U.S. Government Printing Office, Washington D.C., 1964.
  17. National Bureau of Standards, "Tables relating to Mathieu functions, characteristic values, coefficients, and joining factors," Columbia University Press 13, August 1967.
  18. Leeb, Algorithm 537: Characteristic values of Mathieu's differential equation *ACM Trans. Math. Softw.* , 5, pp 112-117, 1979
  19. Alhargan, F. A., "A complete method for the computation of Mathieu characteristic numbers of integer order," *SIAM Rev.* 38, 2, 239-255, 1996".
  20. Shirts, R.B. Algorithm 721: "MTIEU1 and MTIEU2 two subroutines to compute eigenvalues and solutions to Mathieu's differential equation for noninteger and integer order", *ACM Trans. Math. Softw.* , 19, 3, 276-277 1993
  21. Zhang, S. and Jin, J., *Computation of special functions* (John Wiley & Sons, New York, USA, 1996)
  22. Alhargan, F. A., "Algorithms of all Mathieu Functions of integer order", *ACM Trans. Math. Softw.* , 26, pp. 390-407, 2000.
  23. Caorsi, S, Pastorino, M., and Raffetto, M., "Electromagnetic scattering by weakly lossy multilayer elliptic cylinders," *IEEE Trans. On Antennas and Propag.*, vol. 46, no. 11, pp. 1750-1751, 1998.
  24. S. Caorsi, M. Pastorino, and M. Raffetto, "Radar cross section per unit length of a lossy multilayer elliptic cylinder," *Microwave and Optical Technology Letters*, vol. 21, pp. 380-384, 1999.
  25. Hussein, M.I., and Hamid A.-K., "Electromagnetic Scattering by a Lossy Dielectric Cylinder", *J. of Electromagn. Waves and Appl.*, vol. 15, No.11, 1469-1482, 2001.
  26. Ouda, M., Sebak, A., "Scattering from lossy dielectric cylinders using a multifilament current model with impedance boundary conditions," *IEE Proceedings, Microwaves, Antennas and Propagation*, vol. 139, no. 5 , pp. 429–434, Oct. 1992.
  27. Amendola, G., "Application of Mathieu functions to the analysis of radiators conformal to elliptic cylindrical surfaces," *J. of Electromagn. Waves and Appl.*, vol. 13 No.11, 1403-1120, 1999.